Gas transport properties of polysulphones: 3. Comparison of tetramethyl-substituted bisphenols

J. S. McHattie, W. J. Koros and D. R. Paul*

Department of Chemical Engineering, and Center for Polymer Research,
The University of Texas at Austin, Austin, Texas 78712, USA

The gas sorption and transport properties of a series of polysulphones with tetramethyl ring substitution are reported. The results for tetramethylhexafluorobisphenol A polysulphone (TMHFPSF) and tetramethylbisphenol F polysulphone (TMPSF-F) are compared to tetramethylbisphenol A polysulphone (TMPSF) and bisphenol A polysulphone (PSF). The effect of the substituents on chain mobility and chain packing has been related to the gas transport properties. Dynamic mechanical thermal analysis and differential scanning calorimetry were used to judge chain mobility, while X-ray diffraction and free-volume calculations give information about chain packing. Permeability measurements were made for He, H_2, O_2, N_2, CH_4 and CO_2 at 35°C over a range of pressures up to 20 atm. Sorption experiments were also done for N_2, CH_4 and CO_2 under the same conditions. The permeability coefficients of the methyl-substituted polymers rank in the order TMHFPSF $\gg$ TMPSF $>$ TMPSF-F for all of the gases. This is the same order as the unsubstituted materials, hexafluorobisphenol A polysulphone (HFPSF), PSF and bisphenol F polysulphone (PSF-F), which suggests that the effects of tetramethyl substitution are somewhat additive with other structural modifications. Relative gas permeability values are in agreement with relative fractional free-volume values as well as with γ transition temperatures.

(Keywords: polysulphones; permeation; sorption; diffusion; membranes)

INTRODUCTION

An inherent limit to the performance of gas separation membranes is the trade-off between permeability and permselectivity exhibited by most materials that might be used as membranes. A successful strategy for overcoming this limit involves systematically varying polymer structure to restrict intrasegmental mobility and chain packing efficiency[1-6]. Successful examples of this approach are tetramethylbisphenol A polycarbonate (TMPC)[5,6], tetramethylbisphenol A polysulphone (TMPSF)[7,8] and tetramethylhexafluorobisphenol A polycarbonate (TMHFPC)[6]. The tetramethyl substitution simultaneously increases free volume and chain stiffness. When compared to their unsubstituted counterparts, these methyl-substituted polymers are several times more permeable, with no significant loss in selectivity[5-8].

Pilato et al.[7] reported exceptionally high separation factors for TMPSF. More recently, Moe et al.[8] obtained more conservative values for the selectivity of this polymer. The results from the present study agree with those of Moe and coworkers. Much care was taken to obtain these results with special regard to such issues as film preparation, thermal history and removal of residual solvents. Therefore, it is believed that the results of Pilato et al. are in error.

The present work involves the study of a series of tetramethyl-substituted polysulphones in which the

isopropylidene unit of TMPSF has been replaced with another molecular group. The effect of these substitutions on gas transport properties is related to segmental mobility using thermal techniques and to chain packing by free-volume analysis. Tetramethylhexafluorobisphenol A polysulphone (TMHFPSF) and tetramethylbisphenol F polysulphone (TMPSF-F) are compared to TMPSF. Bisphenol A polysulphone (PSF), which has been commercially used in gas separation membranes[9,10], is also included as the baseline unsubstituted material. Chemical structures and other monomer and synthesis information are presented in *Table 1*.
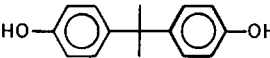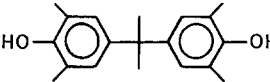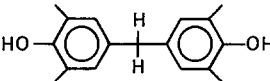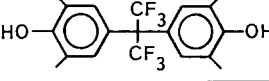
This paper parallels a similar study of polysulphones without the tetramethyl ring substitution[11]. Included in that group are hexafluorobisphenol A polysulphone (HFPSF) and bisphenol F polysulphone (PSF-F), which provide a base for comparison with TMHFPSF and TMPSF-F. Another paper deals with the differences between symmetric and asymmetric methyl substitution of polysulphones[12].
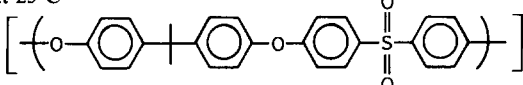
MATERIALS

High-molecular-weight polysulphones were synthesized by the condensation of the appropriate bisphenol and a dihalogenated diphenylsulphone in the presence of a base. One of two procedures, described by Johnson et al.[13] and by Mohanty et al.[14-16], was used with only slight modification[12]. Special care was taken to remove residual solvents, especially 1-methyl-2-pyrrolidinone

---

*To whom correspondence should be addressed

Table 1 Monomer and synthesis information for polysulphones

Bisphenols			Synthesis				
Structure	Source	Recrystallization	Polymer	Method	Time (h)	T ($°C$)	$[\eta]^a$ (dl g^{-1})
HO⟨O⟩—⟨O⟩—OH	Aldrich Chemical Co.	Toluene	PSF[b]	Ref. 13	4	160	0.40
HO⟨O⟩—⟨O⟩—OH	Mitsubishi Gas Chemical Co.	Sublimed	TMPSF	Refs 14–16	16	175	1.06
HO⟨O⟩—H/H—⟨O⟩—OH	Kennedy and Klim Inc.	Sublimed	TMPSF-F	Refs 14–16	30	170	0.45
HO⟨O⟩—CF₃/CF₃—⟨O⟩—OH	Polysciences Inc.	CH_2Cl_2, sublimed	TMHFPSF	Refs 14–16	19	160	0.82

[a] In chloroform at 25°C

[b] The structure is

$$\left[-O-\bigcirc-\bigcirc-O-\bigcirc-\underset{O}{\overset{O}{S}}-\bigcirc- \right]$$

Table 2 Characterization of molecular packing for polysulphones

			Bondi		Sugden	
Polymer	ρ (g cm^{-3})	d-spacing^a (Å)	$V - V_0$ (cm^3 g^{-1})	$(V - V_0)/V$	$V - V_0$ (cm^3 g^{-1})	$(V - V_0)/V$
PSF	1.240	5.0	0.126	0.156	0.106	0.132
TMPSF	1.151	5.5	0.148	0.171	0.131	0.151
TMPSF-F	1.184	5.2	0.138	0.163	0.125	0.148
TMHFPSF	1.286	5.3	0.153	0.196	0.136	0.174

^{a}X-ray diffraction, $\lambda = 1.54$ Å

(NMP), during polymer recovery. This was especially problematic when dealing with these high-T_g polymers, as prolonged exposure to temperatures above T_g resulted in polymer crosslinking and degradation. NMP was removed successfully by Soxhlet extraction[17] for several days each with water and ethanol. Table 1 lists monomer sources and purification techniques as well as the details of the polymerization reactions. Amorphous films of each of the polymers were prepared by casting from methylene chloride on a clean glass plate. The films were then dried thoroughly at 60°C for 1 week in a vacuum oven before characterization. As a measure of molecular weight, the intrinsic viscosity for each polymer was obtained in chloroform at 25°C using a size 25 Cannon–Fenske viscometer.

FREE-VOLUME ANALYSIS

The free volume of each of the polymers was obtained by subtracting a calculated occupied volume, V_0, from the measured specific volume, V. The specific volume was measured by flotation of small samples of film in a density gradient column maintained at 30°C. The specific free volume (SFV) and fractional free volume (FFV) are given by:

$$SFV = V - V_0 \qquad FFV = (V - V_0)/V \qquad (1)$$

The group contribution methods of Bondi[18,19] and of Sugden[20] can be used to calculate V_0. As a complement to the free-volume analysis, wide-angle X-ray diffraction measurements were performed on a Phillips X-ray

diffractometer with Cu K_α radiation having a wavelength of 1.54 Å. The d-spacing, a measure of the most probable intersegmental spacing[21], was calculated from the Bragg equation[22], $n\lambda = 2d \sin \theta$, at the angle of maximum reflective intensity.

The calculated free-volume values and the X-ray diffraction d-spacing for each polymer are given in Table 2. The d-spacing and fractional free volume are larger for the substituted polymers than for PSF. In agreement with the previous study[12], symmetric methyl substitution results in greater interchain distance and more free volume than the unsubstituted polymer. Among the methyl-substituted polymers, the d-spacing is not entirely consistent with the FFV, but the X-ray diffraction patterns are quite broad, making the d-spacing only an approximate measure of molecular packing. The FFV is likely to be a more reliable measure of packing efficiency. As observed in other polycarbonates[23] and poly-sulphones[11,12], FFV based on the Bondi method correlates well with gas permeability. The correlation between the gas permeability and diffusion coefficients and the FFV for the entire family of polysulphones is given in the Appendix.

THERMAL ANALYSIS

The glass transition temperature of each polymer was determined by differential scanning calorimetry with a Perkin–Elmer DSC-7 at a scanning rate of 20°C min^{-1}. The midpoint of the heat capacity shift on the second scan was taken as the T_g. Low-temperature transitions

Table 3 Thermal transitions for polysulphones

Polymer	D.s.c.[a] T_g (°C)	D.m.t.a./110 Hz T_α (°C)	T_β (°C)	T_{γ_1} (°C)	T_{γ_2} (°C)
PSF	186	193	85	–	–80
TMPSF	242	_[b]	–	–10	–92
TMPSF-F	232	_[b]	–	25, –50	–85
TMHFPSF	248	_[b]	–	5, –45	–100

[a] 20°C min^{-1}
[b] Out of range (>200°C)

were examined by dynamic mechanical thermal analysis (d.m.t.a.) using the Imass Autovibron Dynamic Mechanical Viscoelastometer operated in the tensile mode at 110 Hz and at a heating rate of 1°C min^{-1}. These d.s.c. and d.m.t.a. results are summarized in *Table 3*.

Polysulphones and related poly(arylene ether)s exhibit several transition regions in the glassy state, which can be associated with specific molecular phenomena. The transitions are generally labelled with the symbols α, β, γ, etc., in order from high to low temperature, where the α transition corresponds to the glass-to-rubber transition. The glass transition temperature has often been used as the sole measure of polymer chain rigidity, but the secondary transitions may provide some useful information as well. Of particular interest is the low-temperature γ transition. This transition has been attributed to small-scale molecular motions about flexible linkages in the polymer chain[24,25]. Because they are on the scale of the repeat unit or smaller, these motions may be related to the gas transport process. The broad γ transition is most likely a composite of several superimposed peaks associated with the different molecular groups that make up the repeat unit[25–27]. For polymers that are largely aromatic, like these polysulphones, phenylene motions tend to be the most significant contributors to the γ transitions[24,25]. Replacement of phenylene hydrogens with larger molecular groups can shift the γ peaks considerably[12,24].

In a previous paper[12], it was noted that the position of the low-temperature γ_2 transition was related to polymer free volume. The transition occurs at a lower temperature for materials with higher FFV presumably because intermolecularly imposed restraints to small-scale molecular motions are reduced. This peak was ascribed to the motion of the diphenylsulphone portion of the polymer repeat unit, which is the same for each material in this study. The γ_1 peak was associated with the bisphenol half of the repeat unit. For consistency, the same notation is used here. Where two peaks are present due to multiple substitutions, the peaks are labelled as γ_1 and γ_1'.

The tan δ curves from the dynamic mechanical spectra of each of the polysulphones are given in *Figure 1*. The curves are offset vertically with a shift of one order of magnitude between each one. For PSF, only one broad γ peak is present, while two or more peaks appear in the γ region for the methyl-substituted polymers. The position of the γ_2 peak follows the above-mentioned relationship with free volume. The temperature of this peak is the lowest for TMHFPSF, the polymer with the highest FFV, and increases as the free volume decreases. The positions of the γ_1 peaks are complicated by the

intramolecular differences between polymers; however, they seem to follow the same general trend with free volume as the γ_2 transition. The T_g varies in an opposite manner, increasing with FFV. By design, for this set of polymers, the same substitutions that inhibit chain packing also result in a loss of large-scale chain mobility. A more detailed look at the dynamic mechanical thermal behaviour of these and other polysulphones will be presented in a future paper.

GAS SORPTION AND TRANSPORT

Permeation

Pure-gas permeability measurements were made at 35°C for He, H_2, O_2, N_2, CH_4 and CO_2 in that order using the standard permeation techniques employed in this laboratory[28,29]. The permeability data were taken by stepping up from 1 atm with no prior exposure to high-pressure gas. Permeability isotherms are presented as a function of upstream pressure in *Figures 2–7*. In the absence of strong plasticization[28], gas permeability coefficients generally decrease or remain constant with increasing driving pressure. The CO_2 permeability coefficient for TMHFPSF begins to increase above about 15 atm, indicating the onset of plasticization. This phenomenon is a result of the high concentration of sorbed CO_2 in the polymer at the elevated pressures. The permeability coefficients for all gases rank in the order:

$$\text{TMHFPSF} \gg \text{TMPSF} > \text{TMPSF-F} > \text{PSF}$$

This is the same order as their unsubstituted counterparts HFPSF, PSF and PSF-F[11], except that the tetramehtyl-substituted materials are several times more permeable
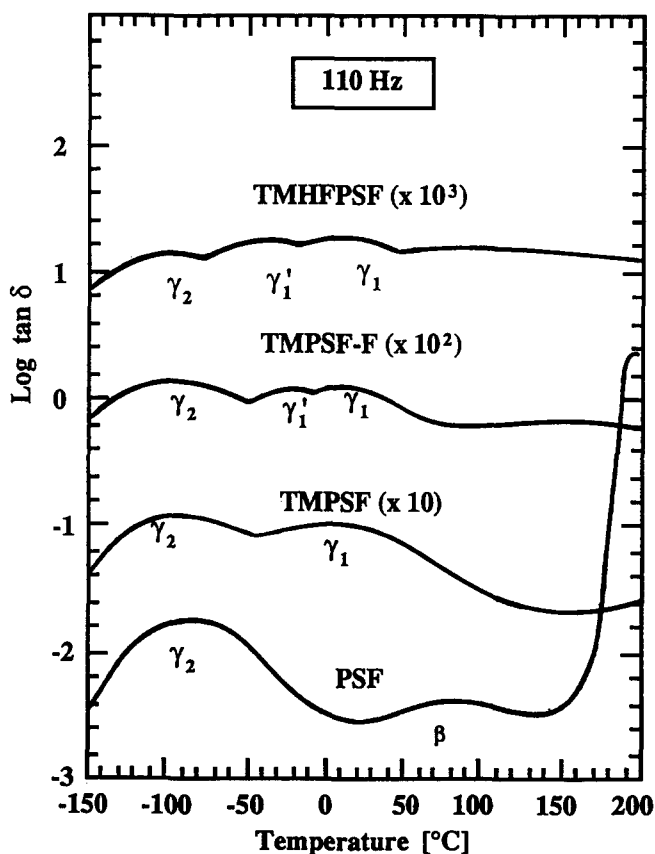
Figure 1 Loss tangent as a function of temperature from dynamic mechanical thermal analysis showing β and γ transitions
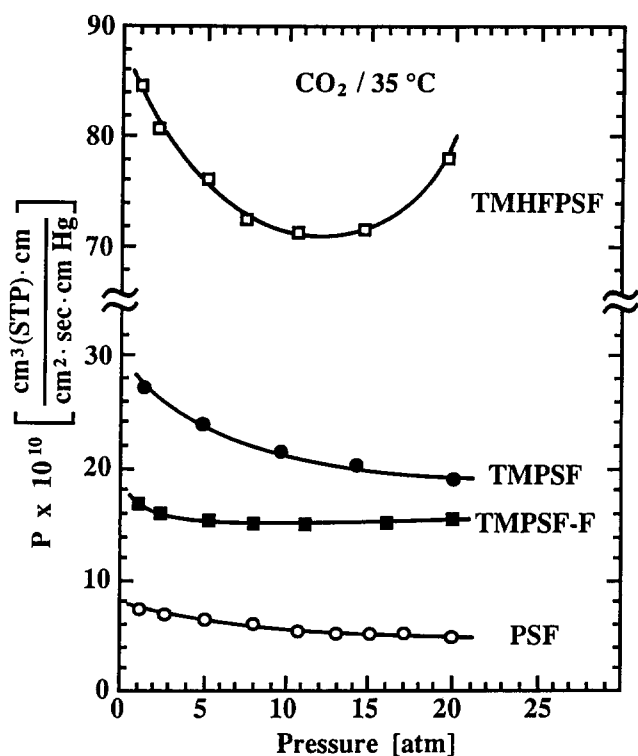
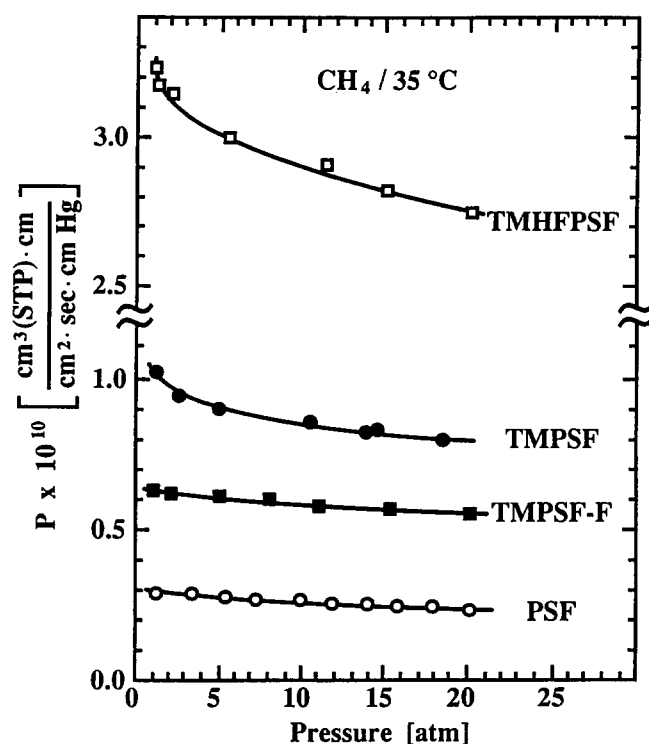Figure 2 Pressure dependence of CO_2 permeability coefficient at 35°C

Figure 3 Pressure dependence of CH_4 permeability coefficient at 35°C

The ideal separation factor, defined as the ratio of the pure component permeabilities:

$$\alpha^*_{AB} = P_A/P_B \qquad (2)$$

provides a useful measure of the intrinsic permselectivity of a membrane material for mixtures of A and B for most cases[28]. The exceptions are instances where strong plasticization is observed, such as for TMHFPSF. Here
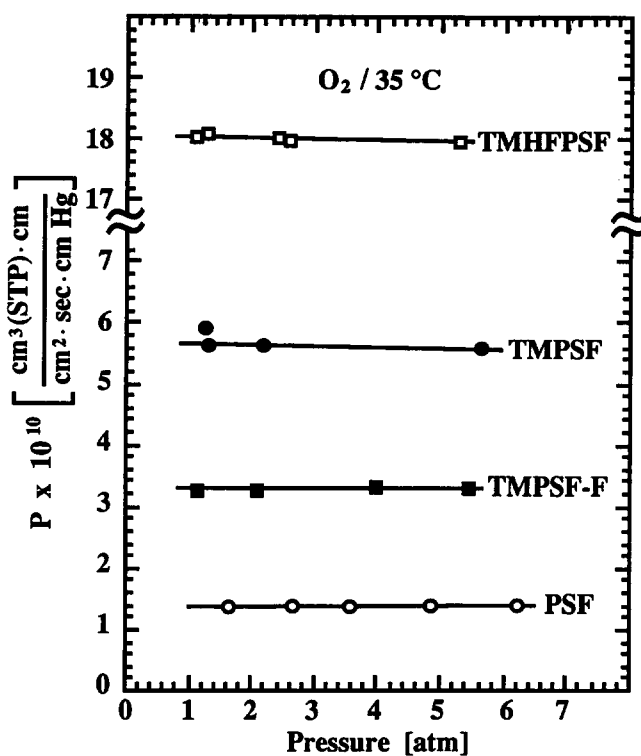

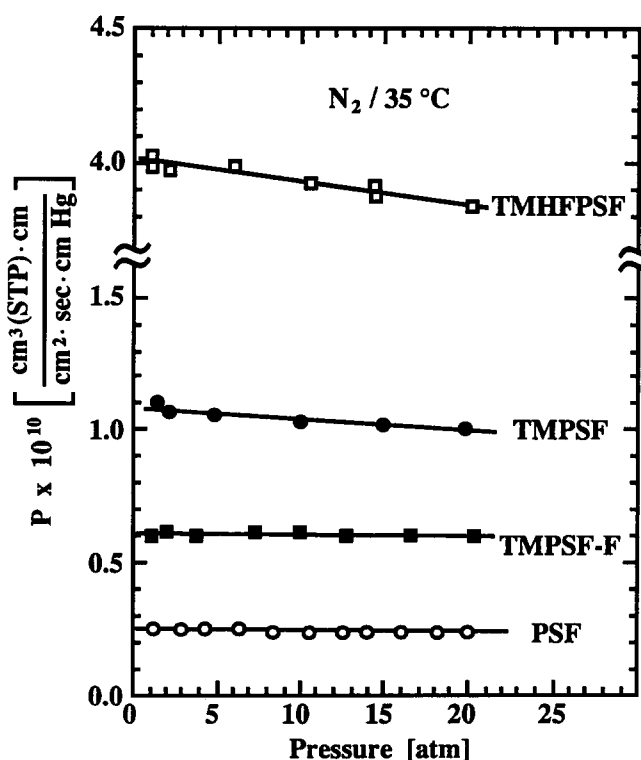Figure 4 Pressure dependence of O_2 permeability coefficient at 35°C

Figure 5 Pressure dependence of N_2 permeability coefficient at 35°C

in each case. These permeability values are in agreement with the relative values for the *FFV* from *Table 2*. As mentioned above, the γ_2 transition temperature is also related to *FFV*. As a result, the γ_2 transition occurs at a lower temperature for the more permeable materials. It is not clear whether there is any real link between the γ-type molecular motions and the gas transport process, but they are related by their sensitivity to free volume.

pure-gas data may be less representative of the mixed-gas performance of the membrane material The permeability coefficients and ideal separation factors for each of the polysulphones at a fixed pressure are shown in *Table 4* for the CO_2/CH_4, O_2/N_2, He/CH_4 and He/H_2 gas pairs. TMPSF is several times more permeable than PSF with little loss in selectivity. The separation factor remains constant for the CO_2/CH_4 gas pair and is decreased slightly for O_2/N_2 and He/CH_4. The high degree of chain stiffness brought about by the methyl substitution may be responsible for this high relative selectivity. The replacement of the isopropylidene group of TMPSF with a hexafluoroisopropylidene unit further increases the permeability, again with only small change in selectivity. Replacement with a methylene unit decreases the permeability somewhat, while increasing the selectivity. These are the same results seen when substituting for the isopropylidene of PSF[11]. This suggests that the effects of the substitutions are, at least to a certain degree, additive.
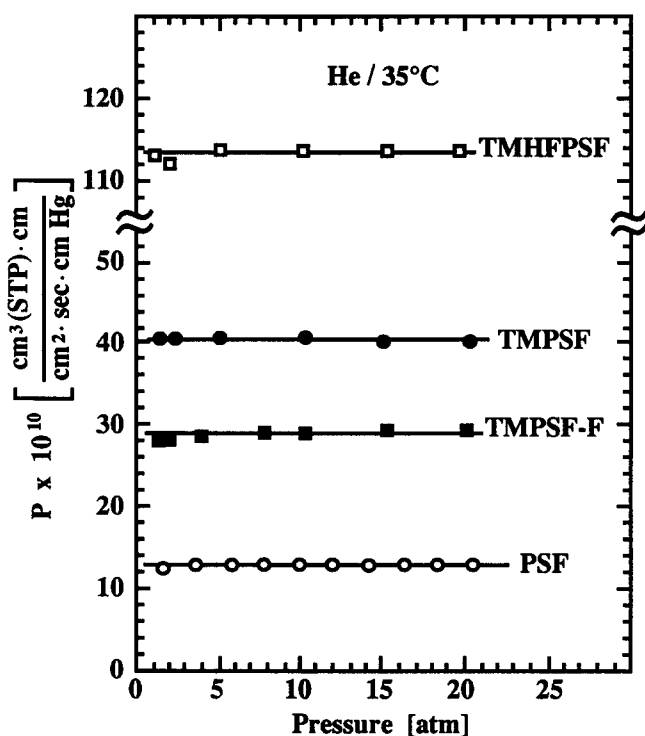
Solubility and diffusivity contributions

Pure-gas sorption measurements using a pressure decay sorption cell[29–31] were made for N_2, CH_4 and CO_2 from 1 to 20 atm at 35°C. Again, the data were taken in this order with no previous exposure to high-pressure gas. Sorption isotherms for TMHFPSF, TMPSF and PSF are shown in *Figures 8–10*. As mentioned above, the high sorption levels for CO_2 in TMHFPSF give rise to plasticization effects. When left under high-pressure CO_2 beyond the usual time required to reach equilibrium, the concentration of sorbed gas continues to rise. This phenomenon has been studied in detail in this laboratory[32–37] but is beyond the scope of this paper.

For the case of negligible downstream pressure, the permeability coefficient can be written as:

$$P = \bar{D}\bar{S} \qquad (3)$$

where $\bar{D}$ is a diffusion coefficient averaged across the membrane thickness, and $\bar{S}$ is a solubility coefficient
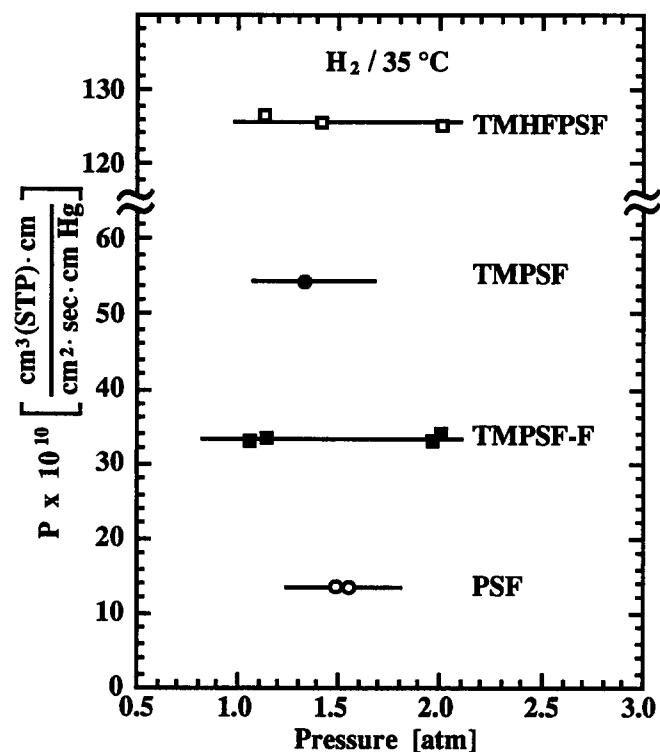

Figure 6 Pressure dependence of He permeability coefficient at 35°C

Figure 7 Pressure dependence of H_2 permeability coefficient at 35°C

Table 4 Permeability and selectivity for polysulphones at 35°C

Polymer	P_{CO_2}[a]	α_{CO_2/CH_4}[a]	P_{O_2}[b]	α_{O_2/N_2}[b]	P_{He}[a]	α_{He/CH_4}[a]	α_{He/H_2}[c]
PSF	5.6	22	1.4	5.6	13	49	0.93
TMPSF	21	22	5.6	5.3	41	45	1.3
TMPSF-F	15	26	3.3	5.4	29	50	0.84
TMHFPSF	72	24	18	4.5	113	38	0.90

$$P \times 10^{10}\left(\frac{cm^3\,(STP)\,cm}{cm^2\,s\,cmHg}\right)$$

[a] 10 atm
[b] 5 atm
[c] 1 atm

obtained from the secant slope of the sorption isotherm at the upstream conditions[38]. An apparent diffusion coefficient can also be estimated from the membrane thickness l and the time lag θ of a transient permeation measurement:

$$D_{app} = l^2/6\theta \qquad (4)$$

The solubility and diffusivity contributions to the permselectivity of each polymer are given in *Table 5* for

the CO_2/CH_4 separation. Values obtained by both methods described above are included for comparison. In general, the apparent solubility obtained from the permeation time lag is larger than the measured solubility coefficient. Both the solubility and diffusion coefficients are increased by the tetramethyl substitution, but the diffusive effect is greater. The mobility selectivity is also much more significant in determining the permselectivity than the solubility selectivity. The solubility selectivity
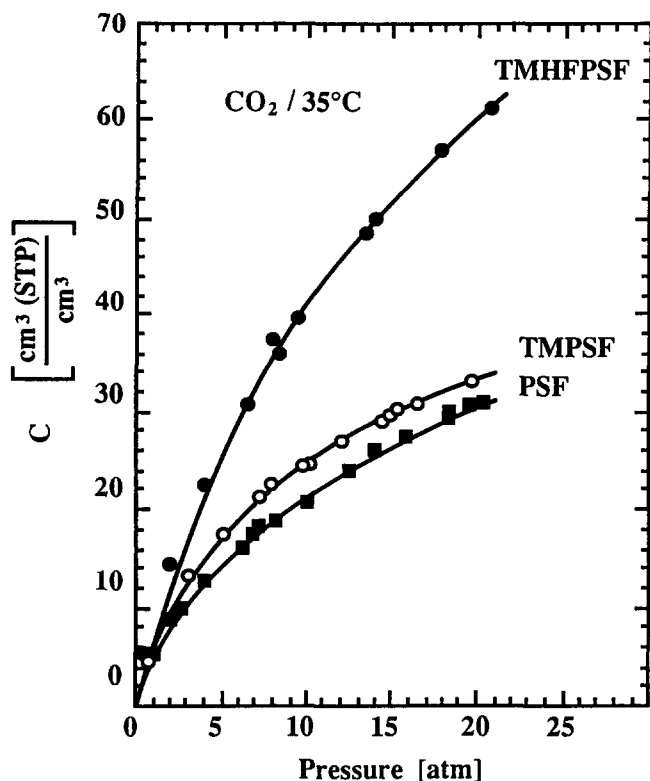

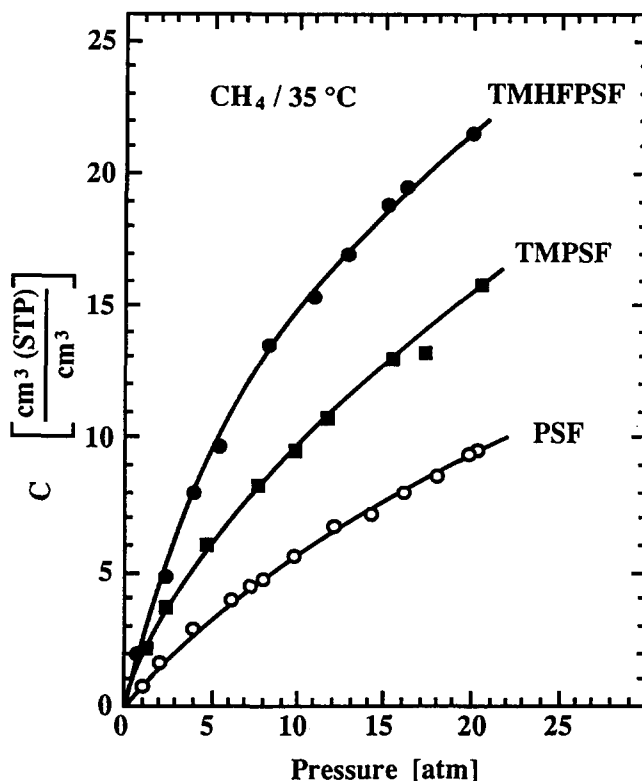**Figure 8** Sorption isotherms for CO_2 at 35°C

Figure 9 Sorption isotherms for CH_4 at 35°C

Table 5 Solubility and diffusivity contributions to CO_2 and CH_4 permselectivity at 10 atm and 35°C[a]

Polymer	P_{CO_2}	$\alpha^*_{CO_2/CH_4}$	S_{CO_2}	$S_{CO_2}/_{CH_4}$	$\bar{D}_{CO_2}$	$\bar{D}_{CO_2}/\bar{D}_{CH_4}$
PSF	5.6	22	2.1(2.1)	3.7 (3.9)	2.0 (2.0)	5.9 (5.6)
TMPSF	21	22	2.5 (3.5)	2.7 (2.4)	6.4 (4.5)	8.1 (9.3)
TMPSF-F	15	22	(4.6)	(2.9)	(2.5)	(7.7)
TMHFPSF	72	24	4.0 (6.1)	2.7 (3.4)	14 (8.9)	8.9 (7.1)

$$P \times 10^{10}\left(\frac{cm^3(STP)cm}{cm^2\,s\,cmHg}\right) \quad S\left(\frac{cm^3(STP)}{cm^3\,atm}\right) \quad D \times 10^8\left(\frac{cm^2}{s}\right)$$

[a] Values in parentheses estimated from permeation time lag

Table 6 Solubility and diffusivity contributions to O_2 and N_2 permselectivity at 5 atm and 35°C

Polymer	P_{O_2}	$\alpha^*_{O_2/N_2}$	$S_{app\,O_2}$	S_{O_2}/S_{N_2}	$D_{app\,O_2}$[a]	D_{O_2}/D_{N_2}
PSF	1.4	5.6	0.24	1.6	4.4	3.6
TMPSF	5.6	5.3	0.53	1.4	8.0	3.8
TMPSF-F	3.3	5.4	0.63	1.4	4.0	3.8
TMHFPSF	18	4.5	0.91	1.4	15	3.3

$$P \times 10^{10}\left(\frac{cm^3(STP)cm}{cm^2\,s\,cmHg}\right) \quad S\left(\frac{cm^3(STP)}{cm^3\,atm}\right) \quad D \times 10^8\left(\frac{cm^2}{s}\right)$$

[a] Estimated from permeation time lag

for each of the substituted polymers is lower than for PSF, but, because the diffusivity selectivities are higher, the overall separation factor is maintained at or above a value of 22 in all cases.

Table 6 gives the solubility and diffusivity contributions for the O_2/N_2 gas pair obtained from equation (4). Again, the tetramethyl substitution has increased both solubility and diffusivity, but the diffusive effects are not large for O_2/N_2 as for CO_2/CH_4. As a result, the separation factor for the O_2/N_2 gas pair is slightly less for the methyl-substituted materials than for their unsubstituted counterparts. The respective O_2/N_2 separation factors for PSF-F and HFPSF are 5.5 and 5.1[11], while those for TMPSF-F and TMHFPSF are 5.4 and 4.5.

Dual mode analysis. Fitting the sorption isotherms from *Figures 8–10* with the dual mode model[39,40]:

$$C = k_D p + \left(\frac{C'_H b}{1 + bp}\right)p \qquad (5)$$
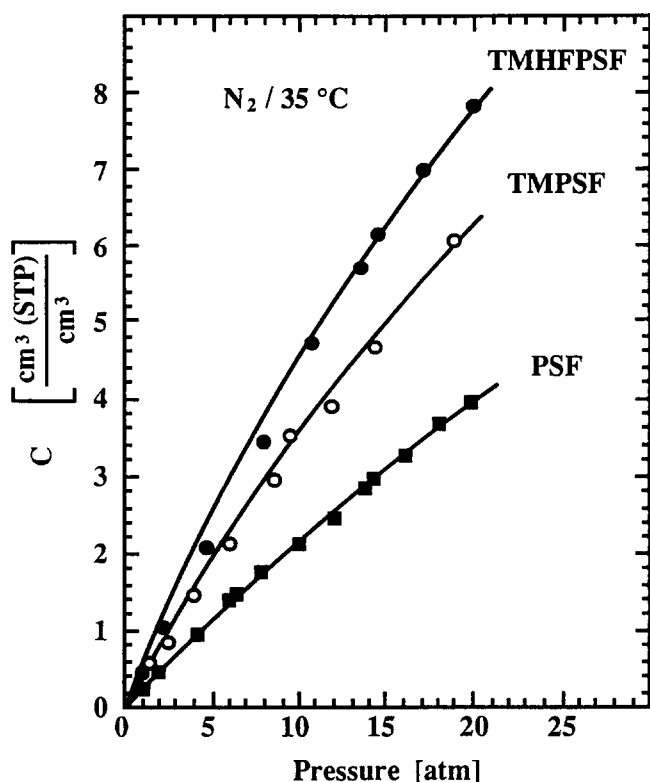
yields the parameters listed in *Table 7*. The parameter

k_D is the Henry's law solubility coefficient, C'_H is the Langmuir sorption capacity and b is an affinity parameter characterizing the ratio of the rate constants for sorption and desorption. The statistical analysis was carried out using a SAS program with the Marquardt least-squares method[41]. According to the dual mobility model[42,43], for the case of negligible downstream pressure, the permeability coefficient can be written as:

$$P = k_D D_D \left(1 + \frac{FK}{1 + bp_2}\right) \qquad (6)$$

with

$$K = C'_H b/k_D \qquad F = D_H/D_D$$

The diffusion coefficient for the Henry's law and Langmuir modes, D_D and D_H, can then be readily calculated from the slope and intercept of an experimental plot of permeability *versus* $1/(1 + bp_2)$. The diffusion coefficients so obtained are given in *Table 7*. The values for TMHFPSF were computed without considering
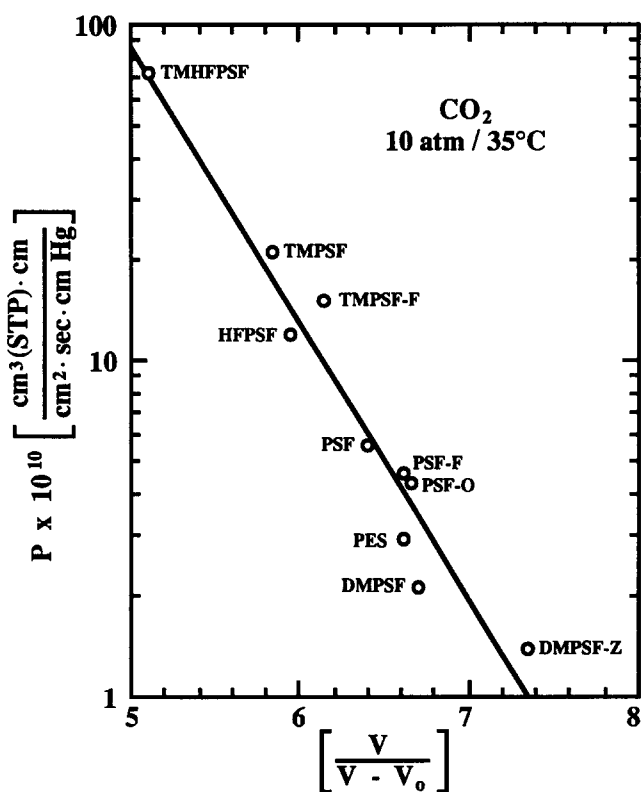

Figure 10 Sorption isotherms for N_2 at 35°C

Figure 11 CO_2 permeability coefficient as a function of Bondi[18,19] fractional free volume for polysulphones

Table 7 Dual mode parameters for polysulphones at 35°C

Polymer	Gas	k_D	C'_H	b (atm^{-1})	D_D	D_H
PSF	CH_4	0.257	6.58	0.0901	0.602	0.131
	CO_2	0.728	19.6	0.260	4.64	0.575
TMPSF	CH_4	0.460	7.26	0.233	1.22	0.159
	CO_2	0.597	26.0	0.261	22.0	1.54
TMHFPSF	CH_4	0.237	26.3	0.0882	7.98	0.257
	CO_2	1.25	46.8	0.155	35.5	2.97

$$k_D\left(\frac{cm^3(STP)}{cm^3\,atm}\right) \qquad C'_H\left(\frac{cm^3(STP)}{cm^3}\right) \qquad D \times 10^8\left(\frac{cm^2}{s}\right)$$
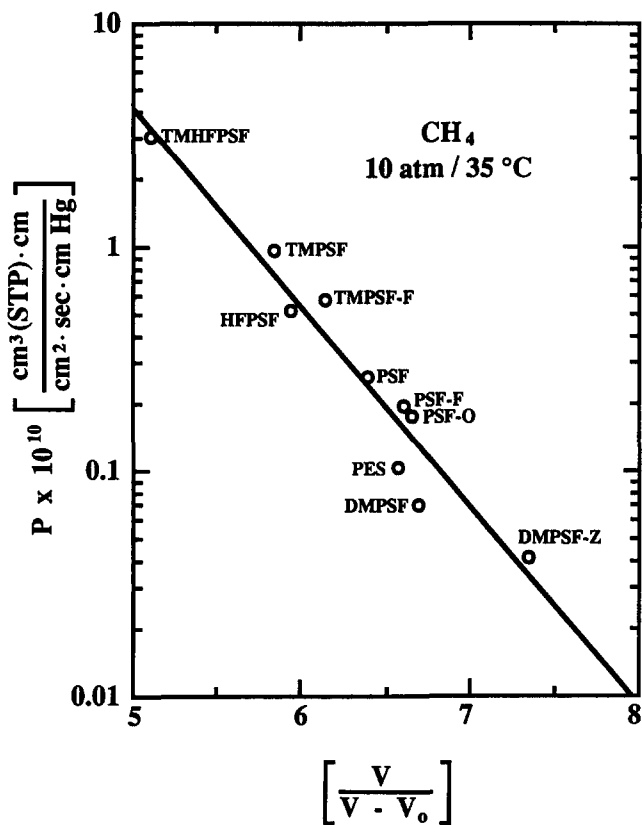
Figure 12 CH_4 permeability coefficient as a function of Bondi[18,19] fractional free volume for polysulphones
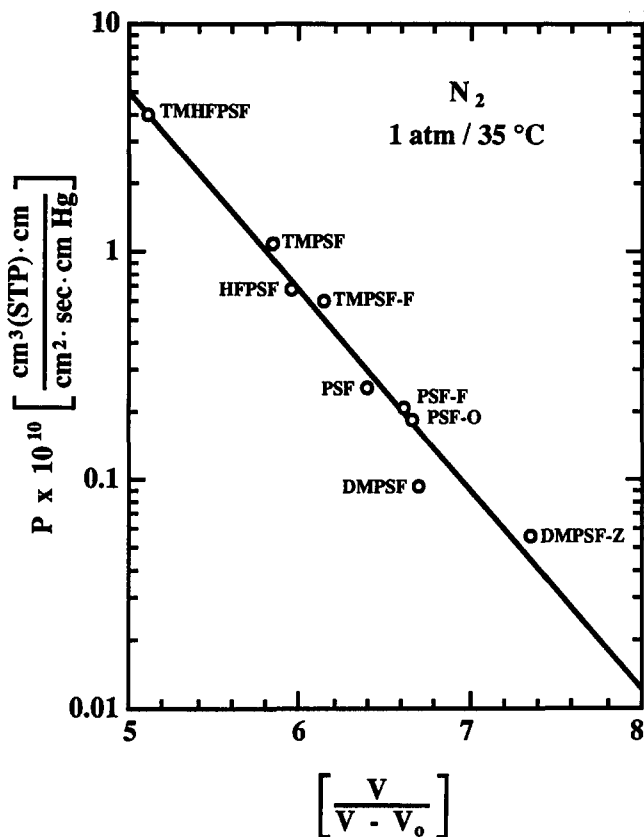

Figure 14 N_2 permeability coefficient as a function of Bondi[18,19] fractional free volume for polysulphones
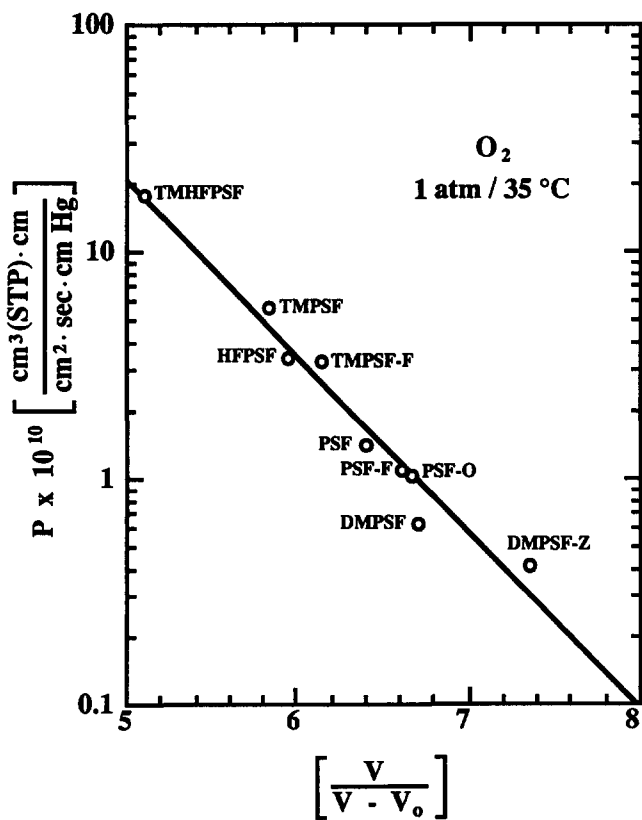

Figure 13 O_2 permeability coefficient as a function of Bondi[18,19] fractional free volume for polysulphones
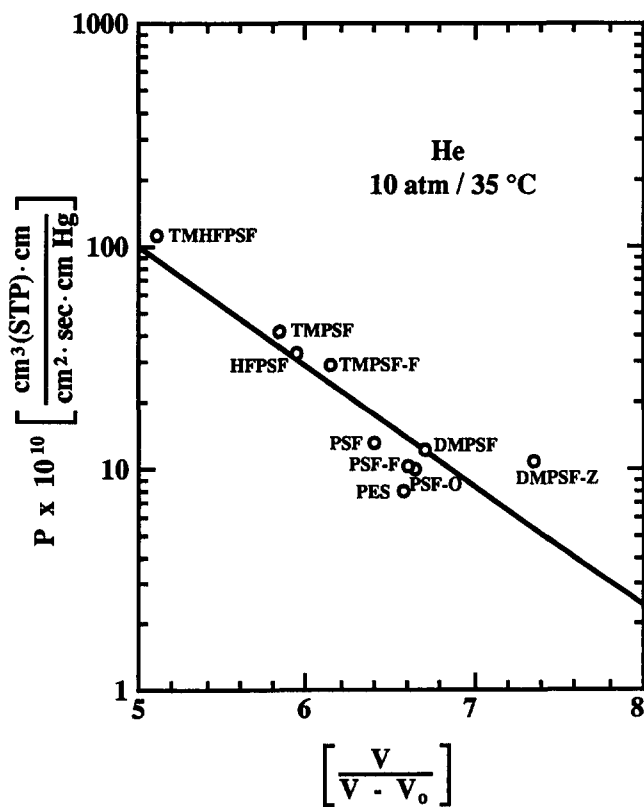

Figure 15 He permeability coefficient as a function of Bondi[18,19] fractional free volume for polysulphones
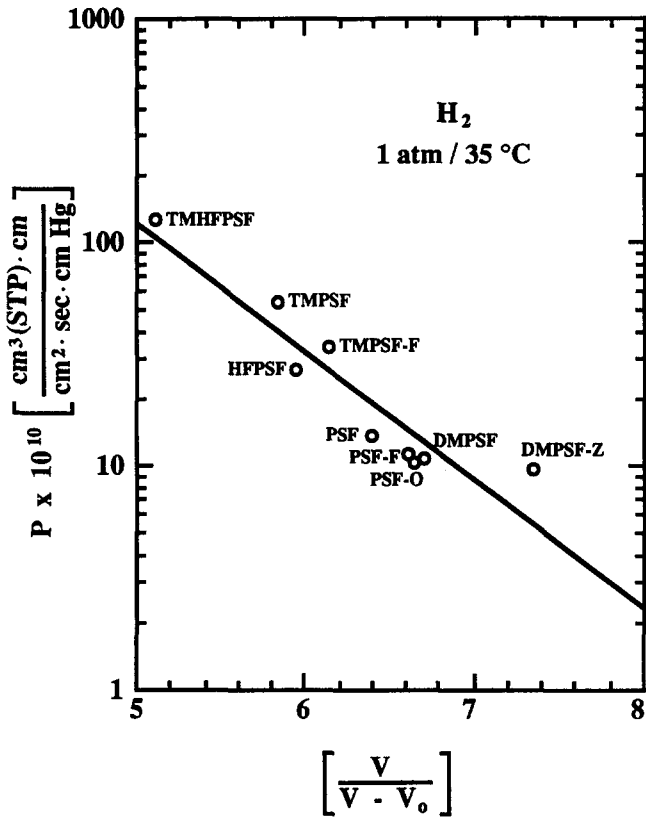
Figure 16 H_2 permeability coefficient as a function of Bondi[18,19] fractional free volume for polysulphones

Figure 17 CO_2 diffusion coefficient as a function of Bondi[18,19] fractional free volume for polysulphones

transport behaviour above 10 atm where significant plasticization begins to be evident for CO_2.

CONCLUSIONS

The symmetric replacement of phenylene hydrogens with methyl substituents in the backbone of bisphenol A polysulphone results in a high degree of chain stiffness
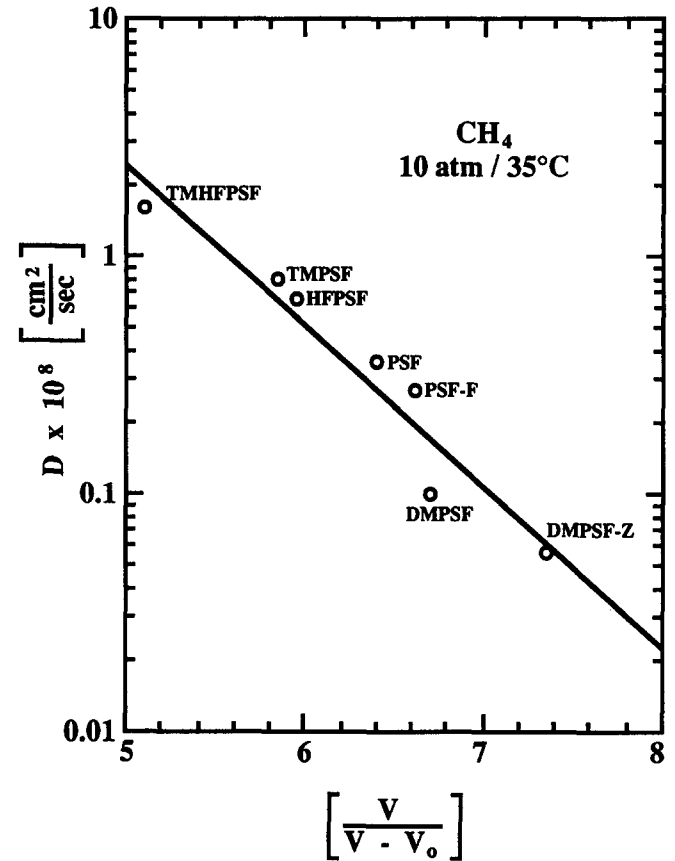

Figure 18 CH_4 diffusion coefficient as a function of Bondi[18,19] fractional free volume for polysulphones
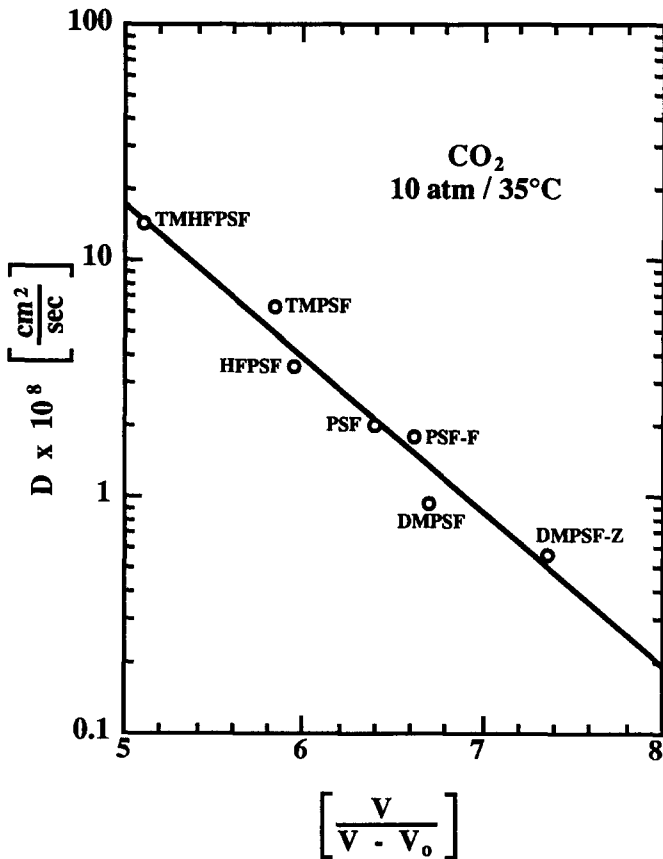
Table 8 Correlation of permeability and diffusion coefficient with fractional free volume $(FFV)^a$ for polysulphones

Gas	A	B	Linear correlation coefficient (R^2)
Permeability			
$CO_2{}^b$	1.08×10^6	1.89	0.940
$CH_4{}^b$	1.14×10^5	2.04	0.937
$O_2{}^c$	1.71×10^5	1.80	0.965
$N_2{}^c$	1.16×10^5	2.01	0.964
He^b	5.32×10^4	1.25	0.818
$H_2{}^c$	8.29×10^4	1.31	0.876
Diffusivity			
$CO_2{}^b$	3.07×10^4	1.50	0.964
$CH_4{}^b$	5.97×10^3	1.56	0.927
$N_2{}^b$	2.43×10^4	1.59	0.970

$$P \times 10^{10} \left(\frac{cm^3\,(STP)\,cm}{cm^2\,s\,cmHg} \right) \qquad D \times 10^8 \left(\frac{cm^2}{s} \right)$$

^{a} Correlations in the form P (or D) $= A \exp(-B/FFV)$
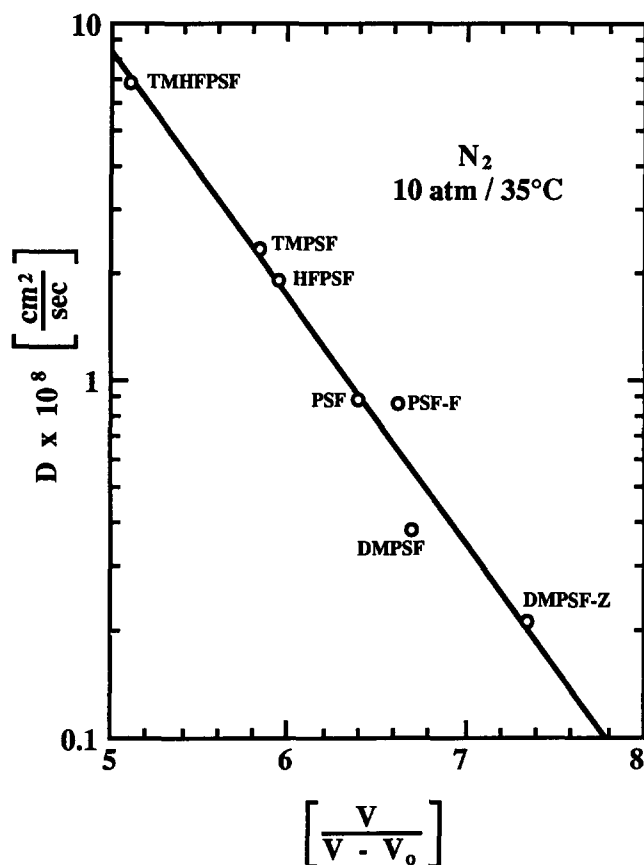^{b} At 10 atm and 35°C
^{c} At 1 atm and 35°C

Figure 19 N_2 diffusion coefficient as a function of Bondi[18,19] fractional free volume for polysulphones

and a relatively open polymer matrix[12]. In this study, the same effect is shown to occur for polysulphones based on other bisphenols. Further, the effects of combined methyl substitution and replacement of the isopropylidene unit of the bisphenol are somewhat additive. TMHFPSF has extremely high permeability while maintaining comparable selectivity to PSF due to this additivity.

As observed previously[12], the relative gas transport rates of these materials correlate with free-volume values calculated from group contribution methods[18-20]. Also, a relationship exists between the position of low-temperature γ transition and gas transport rate. This relationship seems to arise because of their common link with free volume. The barriers to both small-scale polymer motions and penetrant diffusion are affected by free volume in a similar manner.

In designing polymers for gas separations, structural variations that increase chain rigidity while inhibiting chain packing can result in materials with both high permeability and permselectivity. The implications of this study are that it is possible to combine several of these modifications to achieve a desired set of transport characteristics. However, because of the high solubility of gases in polymers with high free volume, like TMHFPSF, plasticization by CO_2 is more prevalent (see *Figure 2*). These plasticization effects may lead to lower actual separation factors in mixed-gas experiments than the values estimated here from pure-gas measurements. Mixed-gas experiments are needed to evaluate more fully the separation characteristics of TMHFPSF, especially for high-pressure mixtures having CO_2 as one of the components.

REFERENCES

1   Pye, D. G., Hoehn, H. H. and Panar, M. *J. Appl. Polym. Sci.* 1976, **20**, 287
2   Kim, T. H., Koros, W. J., Husk, G. R. and O'Brien, K. C. *J. Membr. Sci.* 1982, **37**, 45
3   Kim, T. H., Koros, W. J., Husk, G. R. and O'Brien, K. C. *J. Separ. Sci. Technol.* 1988, **23**, 1611
4   Muruganandam, N., Koros, W. J. and Paul, D. R. *J. Polym. Sci., Polym. Phys. Edn.* 1987, **25**, 1999
5   Muruganandam, N. and Paul, D. R. *J. Membr. Sci.* 1987, **34**, 185
6   Hellums, M. W., Koros, W. J., Husk, G. R. and Paul, D. R. *J. Membr. Sci.* 1989, **46**, 93
7   Pilato, L., Litz, L., Hargitay, B., Osborne, R. C., Farnham, A., Kawakami, J., Fritze, P. and McGrath, J. E. *Polym.Prepr. Am. Chem. Soc., Div. Polym. Chem.* 1975, **16**, 42
8   Moe, M. B., Koros, W. J. and Paul, D. R. *J. Polym. Sci., Polym. Phys. Edn.* 1988, **26**, 1
9   Henis, J. M. S. and Tripodi, M. K. *Separ. Sci. Technol.* 1980, **15**, 1059
10 Lundy, K. A. and Cabasso, I. *Ind. Eng. Chem. Res.* 1989, **28**, 742
11 McHattie, J. S., Koros, W. J. and Paul, D. R. *Polymer* 1991, **32**, 2618
12 McHattie, J. S., Koros, W. J. and Paul, D. R. *Polymer* 1991, **32**, 840
13 Johnson, R. N., Farnham, A. G., Clendinning, R. A., Hale, W. F. and Merriam, C. N. *J. Polym. Sci.* (*A-1*) 1967, **5**, 2375
14 Mohanty, D. K., Hedrick, J. L., Gobetz, K., Johnson, B. C., Yilgor, I., Yilgor, E., Yang, R. and McGrath, J. E. *Polym. Prepr. Am. Chem. Soc., Div. Polym. Chem.* 1982, **23**, 1, 284
15 Mohanty, D. K., Sachdeva, Y., Hedrick, J. L., Wolfe, J. F. and McGrath, J. E. *Polym. Prepr. Am. Chem. Soc. Div. Polym. Chem.* 1984, **25**, 2, 19
16 Mohanty, D. K. PhD Dissertation, Virginia Polytechnic Institute, 1983
17 Mohanty, D. K., Wu, S. D. and McGrath, J. E. *Polym. Prepr. Am. Chem. Soc., Div. Polym. Chem.* 1988, **29**, 1, 352
18 Bondi, A. *J. Phys. Chem.* 1964, 441
19 Bondi, A. 'Physical Properties of Molecular Crystals, Liquids, and Glasses', Wiley, New York, 1968
20 Sugden, S. *J. Chem. Soc.* 1927, 1786
21 Alexander, L. E. 'X-ray Diffraction in Polymer Science', Wiley, New York, 1969
22 Schwarts, L. H. and Cohen, J. B. in 'Diffraction from Materials', Academic Press, New York, 1977, Ch. 3
23 McHattie, J. S., Koros, W. J. and Paul, D. R. *J. Polym. Sci., Polym. Phys. Edn.* 1991, **29**, 731
24 Yee, A. F. and Smith, S. A. *Macromolecules* 1980, **14**, (1), 54
25 Robeson, L. M., Farnham, A. G. and McGrath, J. E. *Midl. Macromol. Monogr.* 1978, **4**, 405
26 Vardarajan, K. and Boyer, R. F. *J. Polym. Sci., Polym. Phys. Edn.* 1982, **20**, 141
27 Chung, C. I. and Sauer, J. A. *J. Polym. Sci.* (*A-2*) 1971, **9**, 1097
28 O'Brien, K. C., Koros, W. J., Barbari, T. A. and Sanders, E. S. *J. Membr. Sci.* 1986, **29**, 229
29 Koros, W. J., Chan, A. H. and Paul, D. R. *J. Membr. Sci.* 1977, **2**, 165
30 Koros, W. J. and Paul, D. R. *J. Polym. Sci., Polym. Phys. Edn.* 1976, **14**, 1903
31 Koros, W. J. PhD Dissertation, The University of Texas at Austin, 1977
32 Jordan, S. M., Koros, W. J. and Beasely, J. K. *J. Membr. Sci.* 1989, **43**, 103
33 Jordan, S. M., Koros, W. J. and Fleming, G. K. *J. Membr. Sci.* 1987, **30**, 191
34 Puleo, A. C., Paul, D. R. and Kelley, S. S. *J. Membr. Sci.* 1989, **47**, 301
35 Raymond, P. C. and Paul, D. R. *J. Polym. Sci., Polym. Phys. Edn.* 1990, **28**, 2079

36   Raymond, P. C. and Paul, D. R. *J. Polym. Sci., Polym. Phys. Edn.* 1990, **28**, 2103
37   Raymond, P. C. and Paul, D. R. *J. Polym. Sci., Polym. Phys. Edn.* 1990, **28**, 2213
38   Chern, R. T., Koros, W. J., Hopfenberg, H. B. and Stannett, V. T. *J. Polym. Sci., Polym. Phys. Edn.* 1984, **22**, 1061
39   Barrer, R. M., Barrie, J. A. and Slater, J. *J. Polym. Sci.* 1958, **27**, 177
40   Vieth, W. R., Howell, J. M. and Hsieh, J. H. *J. Membr. Sci.* 1976, **1**, 177
41   Marquardt, D. W. *J. Soc. Ind. Appl. Math.* 1963, **2**, 431
42   Koros, W. J. and Paul, D. R. *J. Polym. Sci., Polym. Phys. Edn.* 1978, **16**, 1947
43   Petropoulos, J. H. *J. Polym. Sci.* 1970, **8**, 1797

APPENDIX

In a previous paper dealing with structurally modified polycarbonates[23], an attempt was made to correlate gas permeability and diffusivity for a number of polymers with various measures of free volume. Free volume was calculated on both a mass and volume basis by the group contribution methods of Bondi[18,19] and Sugden[20]. The best statistical correlation between free volume and gas permeability coefficient P and gas diffusion coefficient D was found using the volume-based fractional free volume (FFV) computed by the Bondi method. The relation takes the form:

$$P = A \exp(-B/FFV) \qquad (7)$$

or

$$D = A' \exp(-B'/FFV) \qquad (8)$$

where A, A', B and B' are constants for a particular gas.

In the present study, which includes two other papers[11,12], a number of polysulphones have been synthesized and characterized according to their gas transport properties. Plots of gas permeability coefficient for CO_2, CH_4, O_2, N_2, He and H_2 *versus* FFV^{-1} for these materials are given in *Figures 11–16*, respectively. (The abbreviations used here and not already given in the text are: PSF-O, bisphenol O polysulphone; PES, poly(ether sulphone); DMPSF, dimethylbisphenol A polysulphone; DMPSF-Z, dimethylbisphenol Z polysulphone.) The diffusion coefficient for CO_2, CH_4 and N_2 is plotted in the same way with FFV in *Figures 17–19*. The constants from equations (7) and (8) are given in *Table 8* along with the correlation coefficient R^2 of the best-fit line for each graph.

This simple relation between gas permeation and diffusion and free volume fits the data quite well over this limited set of polymers. The lowest value for R^2 is obtained for He and H_2 permeability. These are the smallest gas molecules, so they would tend to be the least sensitive to small changes in free volume. The correlation coefficients are approximately equivalent whether using permeability coefficient or diffusion coefficient as the transport variable.